

Synthesis and application of sodium 2-acrylamido-2-methylpropane sulphonate/*N*-vinylcaprolactam/divinyl benzene as a high-performance viscosifier in water-based drilling fluid

Binqiang Xie,¹ Xiaodong Liu,² Huiqiang Wang,³ Lihui Zheng¹

¹School of Petroleum Engineering, Yangtze University, Hubei 430100, China

²Boxing Company, CNPC, Tianjin 300451, China

³Southwest Oil and Gas Field Company, CNPC, Sichuan 610500, China

Correspondence to: B. Xie (E-mail: Xiebinqiang1981@163.com)

ABSTRACT: Aiming at good thickening ability and temperature resistance in water-based drilling fluid, a novel copolymer viscosifier (SDKP) of sodium 2-acrylamido-2-methylpropane sulfonate (NaAMPS) with *N*-vinylcaprolactam (NVCL) and cross-linking divinylbenzene (DVB) was prepared by micellar radical polymerization. The composition and molecular structure of optimal SDKP under the optimum reaction conditions was characterized by FT-IR, ¹H-NMR, and elemental analysis, and the molecular weight was determined by GPC. Thermal gravimetric analysis showed that the SDKP was even stable when the temperature was not higher than 330 °C. The performance of SDKP as viscosifier for aqueous, brines, and saturated brine bentonite drilling fluid was evaluated before and after aging tests at 230 °C for 16 h. The evaluation results indicated that the SDKP had excellent thickening ability, thermal resistant, and salt tolerance. HTHP rheology test showed that the SDKP containing drilling fluids displayed a thermo-thickening effect in temperature range of 150 to 180 °C, which was beneficial to increase the viscosity and strength of fluids at high temperatures. Shear test showed that the SDKP illustrated a similar shear thinning to xanthan gum. ESEM observations demonstrated that the continuous three-dimensional network was formed in the SDKP aqueous and brines solution, which was probably the main reason for its excellent thickening properties. © 2016 Wiley Periodicals, Inc. *J. Appl. Polym. Sci.* **2016**, *133*, 44140.

KEYWORDS: applications; copolymers; functionalization of polymers; morphology; rheology

Received 9 December 2015; accepted 30 June 2016

DOI: 10.1002/app.44140

INTRODUCTION

The application of water-based drilling fluids was more desirable in areas where oil-based fluids might be restricted due to cost, environmental or logistics constraints.^{1,2} However, as the move was made into high-temperature, high-pressure (HTHP) wells, a main challenge with water-based drilling fluid was related to the thermal degradation of drilling fluid additives, which could lead to rheological instability, filtration-control degradation, etc.^{3–6} These problems, which were critical to the success of any well, might lead to significant accident during drilling operation. Therefore, the choice of proper additives became critical under these conditions and their performance and stability needed to be matched to the HTHP conditions in order to provide proper rheological properties and filtration-control.^{5,6}

Among all drilling fluid additives, the viscosifier (rheology modifier) was crucial in ensuring an appropriate rheological properties which performed a shear-thinning rheology to reduce friction losses and a relatively high low-shear-rate viscosity (LSRV) for

suspending solids (drill cuttings, bridging agent, etc.) and hole cleaning.^{6–8} Some polymers, such as biopolymers^{9,10} (e.g., xanthan gum), could impart the required viscosity profiles of the drilling fluid in drilling operation. However, one of the main problems of these polymers was its poor thermal stability under HTHP conditions.^{5–9} Biopolymers were susceptible to several decomposition pathways at high temperature, including fragmentation, oxidation and hydrolysis reactions, which could lead to significant decreases in rheological properties.^{6–8} This was because that the acetal linkages in polysaccharide backbones of biopolymers were particularly labile at elevated temperature. Therefore, biopolymers were not suitable for HTHP well drilling. Compared with biopolymers, synthetic polymers, such as polyacrylamides and related derivatives,^{11,12} containing carbon-carbon backbones, could provide much better thermal stability and have been available for use as viscosifiers, fluid loss additives, and dispersants.^{5–8} However, synthetic polymers were still susceptible to thermal degradation because of the hydrolysis reactions of amide side chains at elevated temperature.^{4,5} To conquer these defects, extensive

research efforts have been made to reinforce the chain structure of synthetic polymer by incorporation or grafting of thermally stable monomers on the backbone.^{13–18} For instance, 2-acrylamido-2-methyl propane sulfonic acid (AMPS), *N*-vinyl pyrrolidinone (NVP), etc., have been used as thermally stable monomers. Among recent reports on synthetic polymer designed for the HTHP and nearly saturated brine conditions, the stable temperature of modified synthetic polymers was up to 200 °C.^{7,19,20} Despite the advances made in high-temperature synthetic polymer for water-based fluids, the challenge still remained in developing viscosifiers that could meet the higher temperature (in excess of 200 °C, depth of over 6000 m) requirements. Additionally, common synthetic polymers with linear chain often possessed high plastic viscosities and low structural strength, which would not be conducive to producing the desirable suspension properties and shear-thinning properties like biopolymers.⁷ These problems have become the biggest challenge for developing new synthetic polymer viscosifiers.

The utilization of economically feasible and new thermal stable monomers was vital for the preparation of new agents for use in HTHP water-based drilling fluids. Recently, *N*-vinylcaprolactam (NVCL) monomer, which had a similar molecular structure of related NVP, but exhibited a much better hydrolysis resistance at high temperature for its special cyclic amide pendant side,²¹ became industrially available. And it was also suggested that NVCL-based polymers were the family of thermoassociative polymers which displayed a thermoassociating behavior at high temperature.^{22,23} However, there has been reported only for a small number of systems. The aim of the present study was to study the suitability of NVCL as a new structural unit in thermal stable water-soluble polymers for HTHP drilling fluids.

In this context, our main motivation was to develop a high performance polymeric viscosifier which possessed a higher thermal stability (in excess of 230 °C). Meanwhile, the viscosifier should also have excellent shear-thinning property and relatively high structural strength. For this purpose, a new viscosifier (SDKP) was synthesized using AMPS, NVCL, and divinylbenzene (DVB) by the micellar copolymerization technique. The molecular design of this novel viscosifier was as follows: AMPS monomer which had been widely used in oilfield applications for its good thermal and hydrolytic stability and high activity, was chosen to obtain a relatively stiff polymer chain; NVCL monomer was used to improve the rigidity of the copolymer chain and increase the viscosity and structural strength of copolymer containing drilling fluids at high temperature; cross-linking monomer DVB was used to form a micro-crosslinked polymer conformation which was assumed to improve the viscosity and structural strength of drilling fluids. The SDKP synthesized in this article showed excellent thermal stability in water-based fluids (up to 230 °C), and exhibited a better thickening efficiency than HE300 (representative viscosifier of Chevron Phillips Chemical Company) and a similar shear thinning property to xanthan gum.

EXPERIMENTAL

Materials

2-Acrylamido-2-methylpropanesulphonic acid (AMPS, 99%) from Suyuan Chemicals (Weifang, China) was recrystallized from

methanol. *N*-vinylcaprolactam (NVCL, 98%) from Aote Chemicals (Zibo, China) was distilled under reduced pressure. 2,2-Azobisisobutyronitrile (AIBN) from Kemao Chemicals (Tianjin, China) was recrystallized from ethanol and used as initiator. Divinyl benzene (DVB), sodium hydroxide (NaOH), sodium dodecylsulfate (SDS) and acetone, from Sinopharm Chemicals (Shanghai, China), were analytical reagent. Viscosifier HE300 (100%, solid powder) from Chevron Phillips Chemicals. Xanthan gum (99.5%, solid powder) from Zibo Deosen Chemicals (Zibo, China).

Synthesis of SDKP

SDKP samples were synthesized by micellar free radical polymerization utilizing sodium dodecylsulfate as the surfactant. Comonomers of AMPS, NVCL, and DVB were dissolved in deionized water with stirring. The pH value of the mixed solution was adjusted to between 7.0 and 8.0 by adding sodium hydroxide solution. Then, the mixed solution and SDS was added into a reaction flask and deoxygenated with nitrogen. After heating to the desired temperature, the initiator (AIBN) was added to the reaction mixture. The polymerization was kept 6 h at the reaction temperature. The reaction product was precipitated by acetone, and washed by mixture of acetone and water for many times. The product was dried under vacuum at 60 °C for 2 days. The chemical structure of SDKP was shown in Figure 1. PAD (without NVCL monomer) samples were prepared using the same synthetic method.

Characterization of SDKP

FT-IR spectra of SDKP was conducted with NICOLET-710 FT-IR spectrophotometer (USA) in the range 4000 to 500 cm^{-1} using solid state KBr disc technique. ¹H-NMR spectra of SDKP was characterized with 600 MHz Varian Inova spectrometer (USA) in D₂O. The elemental analysis of SDKP was conducted by CARLO ESRA-1106 elemental analyzer (Italy) to determine carbon, nitrogen, and sulfur content. Molecular weights (M_w) of SDKP were determined by Waters 2695 gel permeation chromatographic. NaNO₃ aqueous solution was used as an eluent. The SDKP solution was filtered through a 5 μm filter before it was injected into the column. And Pullulan p-82 was used for an initial calibration of the column. The column temperature was kept at 30 °C and the flow rate of injection was fixed at 1.0 mL/min. Thermogravimetric analysis (TGA) of SDKP was carried out with HTG-1 (China) thermal analyzer under nitrogen flow (100 mL/min). The temperature range was from 15 to 600 °C at a heating rate of 10 °C /min.

Drilling Fluid Preparation and Hot Rolling Tests

The low-solid freshwater base fluid (LSFBF) was made up by maintaining the ratio of the bentonite (Weifang Huawei Bentonite, China), H₂O, and Na₂CO₃ at 3.0:100.0:0.2 by weight. Before use, the base fluid was stirred at high speed for about 20 min and aged for 24 h at room temperature to hydrate the bentonite. Two types of low-solid brine fluids were made of 3.0% of sodium bentonite, 8.0% of NaCl or saturated brine (36.0% NaCl), and 0.2% of Na₂CO₃. The preparation procedure was similar to that of the LSFBF.

Hot rolling tests of drilling fluids were carried out in a GW300-type rolling oven (Qingdao Hantongda Petroleum instrument,

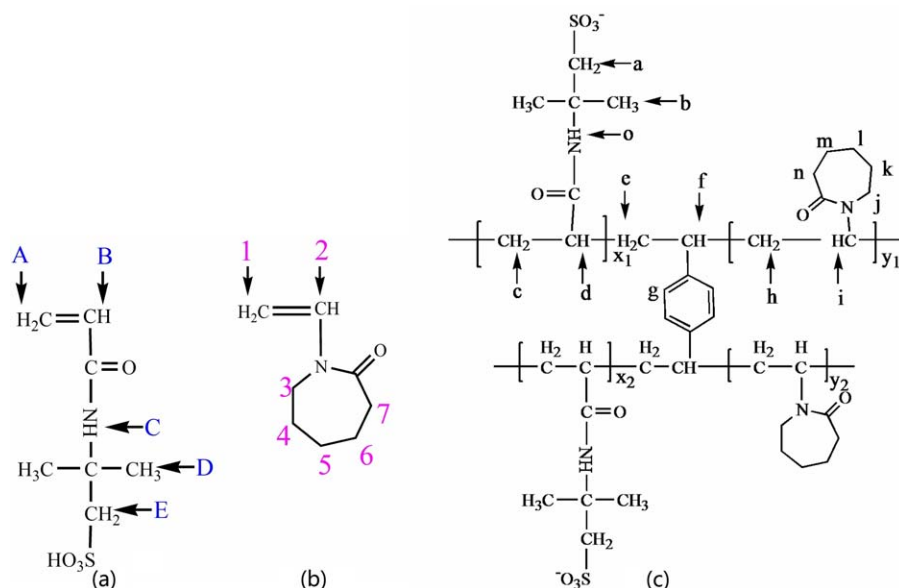


Figure 1. Chemical structure of AMPS, NVCL, and SDKP. [Color figure can be viewed in the online issue, which is available at wileyonlinelibrary.com.]

China) through hot rolling at appointed temperature for 16 h. Then the fluids were cool to room temperature and fluids performance tests were conducted.

Fluid Performance Test

Drilling fluids performance tests were conducted according to the American Petroleum Institute (API) specifications. Rheological properties were measured before and after hot rolling aging tests using a ZNN-D6-type rotating viscometer (Qingdao Haitongda Petroleum instrument, China) at room temperature. The rheological parameters such as apparent viscosity (AV, mPa s), plastic viscosity (PV, mPa s), yield point (YP, Pa), and gel strength (Gel, Pa) including initial gel strength 10 s (Gel10s) and final gel strength 10 min (Gel10min) could be calculated using the following formula:

$$AV = 0.5 \times \varphi_{600} \quad (1)$$

$$PV = \varphi_{600} - \varphi_{300} \quad (2)$$

$$YP = 0.511 \times (\varphi_{300} - PV) \quad (3)$$

$$Gel = 0.5 \times \varphi_{3 \text{ max}} \quad (4)$$

AV was defined as the viscosity of the fluid that exhibited the shear stress at a shear rate of 600 rpm. PV which was a measure of the high shear rate viscosity of the fluid, was defined as the shear stress in excess of the yield stress that would induce unit rate of shear. YP which was a measure of the yield stress of the fluid, was defined as the shear stress of the fluid at laminar flow. Gel strength which was an indication of ability to suspend mud solids, was defined as the space frame structure strength of the fluid formed in a stationary state. Gel strength was closely related to the length of time.

Before testing gel strength, the fluid must be stirred for a predetermined time in order to avoid precipitation. The measured Gel10s or Gel10min of a fluid was half of the maximum reading taken from a ZNN-D6-type viscometer at 3 rpm rotational speeds after the fluid has been kept under static conditions for 10 s or 10 min.

The API filtrate volume (FL_{API}) and the high-temperature and high-pressure filtrate volume (FL_{HTHP}) of the drilling fluids was determined with a ZNS-2A-type medium-pressure filtration apparatus (Qingdao Haitongda Petroleum instrument, China) and a GGS42-1-type high-temperature and high-pressure filtration apparatus (Qingdao Haitongda Petroleum instrument, China), respectively. The FL_{API} and FL_{HTHP} were conducted at 25 °C, 0.7 MPa, and 160 °C, 3.5 MPa, respectively.

The rheological parameters at different high temperature (150 °C, 180 °C, 220 °C) and high pressure (4.5 MPa) were measured with a HAAKE RS6000 rheometer (HAAKE Technology Company, Germany).

The shear-thinning properties of 1.0% (mass fraction) SDKP and 1.0% xanthan gum solution were also determined with a HAAKE RS6000 rheometer (HAAKE Technology Company, Germany) by measuring the apparent viscosities at room temperature across a wide shear rate spectrum (0.1–400 S^{-1}).

Environmental Scanning Electron Microscope (ESEM)

Analysis

The microscopic morphology of the SDKP molecules in aqueous and brine solutions was observed by ESEM Quanta450 (FEI). The SDKP solution sample was put directly into the sample room where it was maintained at a certain temperature and pressure to keep the sample at solution conditions during the whole observation.²⁴

RESULTS AND DISCUSSION

Effect of NVCL Amount on the Temperature-Resistance of Polymeric Drilling Fluids

Five different polymer samples were prepared via micellar free radical copolymerization under identical condition except for the feed amount of NVCL. The polymerization conditions, composition, and properties of the samples were shown in Tables I and II. Table I illustrated that the molar compositions of NVCL in samples were higher than the corresponding monomer feed compositions, which

Table I. Feed Composition, Elemental Composition, and Product Composition of Polymers

Sample	Feed molar composition ^a M1:M2:M3	Elemental composition (wt %)			Polymer molar composition M1:M2:M3
		C	N	S	
PAD	99.00:1.00:0.00	—	—	—	—
SDKP1	79.00:1.00:20.00	37.82	6.13	11.45	81.60:0.15:18.25
SDKP2	59.00:1.00:40.00	39.79	6.29	9.15	63.54:0.16:36.30
SDKP3	39.00:1.00:60.00	40.86	6.39	8.03	54.92:0.10:44.98
SDKP4	19.00:1.00:80.00	42.95	6.57	5.80	38.57:0.13:61.30

^aM1:NaAMPS; M2:DVB; M3:NVCL.

was probably due to the low reactivity of NVCL compared to other monomers.^{25–27} Figure 2 showed the gel permeation chromatographic curves of samples. Molecular weights of samples were illustrated in Table III. With increasing NVCL feed amount from 0 to 60 mol %, the molecular weight of samples increased. However, when the NVCL feed amount was up to 80 mol %, the molecular weight of SDKP4 sample decreased obviously, which was probably due to steric effects of excessive NVCL dosage. SDKP3 sample with 60 mol % NVCL had the highest molecular weight.

A series of low-solid freshwater drilling fluids composed of the LSFBF and 0.8% (mass fraction) copolymer samples were prepared, and the effect of NVCL amount on the rheological properties of the low-solid fresh water drilling fluid was measured before and after thermal aging tests at 230 °C for 16 h. The results were illustrated in Table IV.

Compared with PAD, the low-solid drilling fluids with SDKP showed higher retention of all the rheological parameters, including AV, PV, YP, LSRV(φ_3), and gel strength after thermal aging tests. And the retention of all the rheological parameters was further improved with the increase of NVCL amount in the synthesis of copolymers, generally. These results illustrated that the addition of NVCL constitutional units in copolymer could significantly improve the heat resistance of fluids. This was because that NVCL containing special cyclic amide pendant side had a much better thermal stability, and could significantly improve the rigidity of the copolymer chain.²¹ As shown in Table IV, all the rheological parameters value increased gradually as the NVCL mole fraction increased. This phenomenon could be explained as follows: NVCL monomer had a considerable

hydrophobicity, the hydrophobic associations of caprolactam (CL) units were enhanced with increasing NVCL amount, leading to an obvious increase in the rheological parameters of fluids.²³ However, too high NVCL amount would lead to poor solubility and low molecular weight due to steric effects, resulting in the decrease of viscosity and strength. When the copolymers containing CL units was exposed to the higher temperature, although CL units could also occur high temperature degradation, the degradation of CL units would produce a secondary amine structure on the backbone of the copolymer, along with a six carbon chain terminated by a carboxyl.²¹ This structure resulted in a greater molecular volume of the copolymer in fluid, leading to the increase of viscosity and strength of fluid. Because both the rheological parameters value and the retention of the rheological parameters of copolymer with 60 mol % NVCL (by mole of total monomer) behave well, the copolymer with 60 mol % NVCL (by mole of total monomer) was chosen to study further.

Optimum Synthesis Conditions of Viscosifier

Experimental parameters in synthesis of copolymer, such as, initiator amount, reaction temperature, monomer ratio, SDS concentration, pH, etc., had an important influence on the molecular weight and molecular structure of copolymer, which would further affect its rheological performance in the drilling fluid. Adopting the error analysis method and studying the factors affecting these indexes, an orthogonal $L_{16}(4^5)$ test design was used for further optimization of experimental parameters.^{28,29} The stoichiometric numbers of the orthogonal experiment was shown in Table V in which five key parameters

Table II. Synthesis Conditions, Yield, and Molecular Weights of Polymers

Sample	Reaction conditions			Yield (%)
	w (AIBN) % ^a	w (monomer) % ^b	w (SDS) % ^c	
PAD	0.28	10.00	2.00	93.60
SDKP1	0.28	10.00	2.00	83.20
SDKP2	0.28	10.00	2.00	78.62
SDKP3	0.28	10.00	2.00	80.55
SDKP4	0.28	10.00	2.00	82.13

^aMass fraction relative to total monomer.

^bMass fraction of total monomer.

^cMass percent of SDS in water.

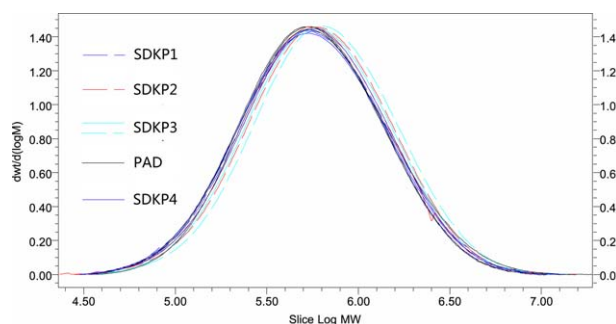


Figure 2. Gel permeation chromatographic curves of polymer samples. [Color figure can be viewed in the online issue, which is available at wileyonlinelibrary.com.]

Table III. Molecular Weights and Polydispersity of Polymers

Sample	M_n	M_w	Polydispersity
PAD	373,400	552,358	1.479263
SDKP1	429,941	634,165	1.475004
SDKP2	588,818	863,579	1.466631
SDKP3	616,408	899,272	1.458890
SDKP4	455,261	675,363	1.483463

including initiator amount (*A*), reaction temperature (*B*), monomer ratio (*C*), surfactant (SDS) amount (*D*), and pH (*E*), were selected. Because the research involved multiobjective optimization, the best optimum synthesis condition was identified according to the two key rheological parameters including YP (an indication of ability to form a space frame structure at motion state) and YP/PV (an indication of shear-thinning ability), of LSFBF with copolymer (0.8% wt) and Na₂SO₃ (0.5% wt) after aging tests. The YP and YP/PV were normalized, and each was given a 50% weight factor. The detailed procedure was as follows,

$$F = (YP - YP_{\min}) / (YP_{\max} - YP_{\min}) \quad (5)$$

$$G = [(YP/PV) - (YP/PV)_{\min}] / [(YP/PV)_{\max} - (YP/PV)_{\min}] \quad (6)$$

$$H = 50\%F + 50\%G \quad (7)$$

The bigger the *H* value was, the bigger YP and YP/PV would be. According to the orthogonal experiment, the bigger R^X , the more significant influence of *X* on experimental results (*X* could be *A*, *B*, *C*, *D*, or *E*). The orthogonal design experiment result was illustrated in Table VI. According to *R* values, the effect on the *H* value of SDKP decreased in the order: $B > A > C > D > E$. According to the orthogonal experiment, the bigger K_i^X (*X* could be *A*, *B*, *C*, *D*, or *E*, and *i* could be 1, 2, 3, or 4), the better experimental result under the X_i condition. And the

optimum synthesis conditions were shown in Table VII. As listed in Table VII, the performance of SDKP under the optimum conditions was better than the experiment result under other test conditions. Therefore, the SDKP was synthesized under this optimum synthesis conditions for other experiments.

FT-IR Spectra of SDKP

Figure 3 showed the FT-IR spectra of NVCL, AMPS, and SDKP. Compared with NVCL and AMPS, the stretching vibration of C-H of vinyl at about 3070 cm⁻¹ was disappeared in the spectra of SDKP, which indicated that SDKP did not contain unreacted monomers. Compared with AMPS, the spectra of SDKP showed a strong stretching vibration peak of -CH₂ at 2940 cm⁻¹, which indicated the high content of methylene in SDKP. Compared with NVCL, the spectra of SDKP showed the characteristic absorption peaks of -SO₃⁻ at 1040 cm⁻¹ and 1195 cm⁻¹, which indicated the incorporation of AMPS into the SDKP. The spectra of SDKP showed the bending vibration absorption of -CH, -CH₃, -CH₂ at 1290 cm⁻¹, 1401 cm⁻¹, 1440 cm⁻¹, respectively, a bend vibration peaks of C-N at 1540 cm⁻¹, a stretching vibration peaks of C=O at 1670 cm⁻¹, a stretching vibration peak of -CH₂ at 2940 cm⁻¹, a stretching vibration peak of N-H at 3430 cm⁻¹. However, because of the small amount of DVB amount, the incorporation of DVB into the SDKP could not be detected.

¹H-NMR Spectra of SDKP

The ¹H-NMR spectrum of SDKP in D₂O was shown in Figure 4. The spectrum of NVCL and AMPS was used as a comparison. Compared with AMPS and NVCL, the spectra of SDKP showed relatively broad peaks due to polymer chains of varying lengths. Compared with AMPS and NVCL, the broad peak at 7.514 ppm could be assigned to the protons of phenyl of DVB, which indicated the successful incorporation of DVB into the SDKP. All the resonances of protons of SDKP were as follows,

Table IV. Effect of NVCL Amount on the Properties of SDKP

Fluid formulation	Hot rolling test	Typical rheological parameters					
		φ3	AV (mPa·s)	PV (mPa·s)	YP (mPa·s)	YP/PV	G _{10s} /G _{10min}
LSFBF + 0.8% PAD + 0.5% Na ₂ SO ₃	Before	1.0	19.0	16.0	3.0	0.19	0.5/0.75
	After	0.5	11.0	9.0	1.5	0.17	0.25/0.5
	Retention (%)	50.0	57.9	56.3	50.0	-	-
LSFBF + 0.8% SDKP1 + 0.5% Na ₂ SO ₃	Before	3.0	34.0	23.0	11.0	0.43	1.5/2.0
	After	1.5	22.5	16.0	6.5	0.29	1.0/1.25
	Retention (%)	50.0	66.2	69.6	59.1	-	-
LSFBF + 0.8% SDKP2 + 0.5% Na ₂ SO ₃	Before	3.5	43.0	34.0	11.0	0.32	1.5/2.5
	After	2.0	30.0	24.0	5.0	0.20	1.0/2.0
	Retention (%)	57.1	69.8	70.6	45.4	-	-
LSFBF + 0.8% SDKP3 + 0.5% Na ₂ SO ₃	Before	4.5	45.5	32.0	13.5	0.42	2.25/3.0
	After	3.0	31.5	25.0	7.5	0.30	1.5/2.0
	Retention (%)	66.7	69.2	78.1	55.6	-	-
LSFBF + 0.8% SDKP4 + 0.5% Na ₂ SO ₃	Before	3.0	40.0	30.0	10.0	0.33	1.5/2.0
	After	2.0	28.0	22.0	5.0	0.23	1.0/1.25
	Retention (%)	66.7	70.0	73.3	50	-	-

Table V. Factor and Levels for Orthogonal Experiment

Level	A Initiator concentration (%)	B Reaction temperature (°C)	C Mole ratio of NVCL/AMPS/DVB	D SDS concentration (%)	E pH
1	0.10	55	60.0:39.0:1.0	0.5	4
2	0.15	60	60.0:38.7:1.3	1.0	7
3	0.20	65	60.0:38.4:1.6	1.5	10
4	0.25	70	60.0:38.0:2.0	2.0	13

—CH protons of phenyl, δ 7.514 ppm; —CH₂ of AMPS side chain and —CH₂ (*k*) of NVCL side chain, δ 4.202 ppm; —CH protons of NVCL main chain, —NH protons of AMPS side chain, —CH₂ (*j*) protons of NVCL side chain, δ 3.152 ppm; —CH of DVB main chain and —CH of AMPS main chain, —CH₂ (*n*) of NVCL side chain, δ 2.378 ppm; —CH₂ of AMPS main chain, —CH₂ of DVB main chain, —CH₂ of NVCL main chain and —CH₂ (*l, m*) of NVCL side chain, —CH₃ of NaAMPS side chain, δ 1.362 ppm. All the resonances of protons of AMPS, NVCL, and SDKP were shown in Figures 1 and 4. The ¹H-NMR spectrum affirmed the successful copolymerization of AMPS, NVCL, and DVB.

Thermal Analysis

The thermal analysis curve was used to check the performance of polymer under high temperature. The TGA curves of SDKP and

HE300 was shown in Figure 5. The SDKP exhibited three stages of the decomposition. The first thermal decomposition region was below 150 °C, where a little mass loss rate of about 10% was registered. This mass loss should be the water elimination of the copolymers. The temperature range of 150 to 330 °C could be considered without weight loss, because it was too small to consider. The thermal decomposition of SDKP became appreciable at temperatures higher than 330 °C, where the mass loss rate was more than 50%. The second region occurred in the range of 330 to 350 °C, where the mass loss rate was more than 25%. This stage corresponded to the degradation of sulfonic groups. The third region was above 350 °C, where the mass loss rate was more than 25%. This stage corresponded to the decomposition of the polymer backbone. In contrast with SDKP, the HE300 showed appreciable thermal decomposition at a temperature close to 300 °C, which indicated that the SDKP had better heat resistance.

Table VI. Analysis of L₁₆ (4⁵) Orthogonal Design Test Result

Test no.	A	B	C	D	E	YP	YP/PV	H
1	A1	B1	C1	D1	E1	4.5	0.19	0.06
2	A1	B2	C2	D2	E2	6.5	0.26	0.4
3	A1	B3	C3	D3	E3	7.5	0.31	0.6
4	A1	B4	C4	D4	E4	6.0	0.25	0.33
5	A2	B1	C2	D3	E4	5.0	0.18	0.09
6	A2	B2	C1	D4	E3	8.0	0.36	0.75
7	A2	B3	C4	D1	E2	7.5	0.33	0.64
8	A2	B4	C3	D2	E1	6.5	0.23	0.34
9	A3	B1	C3	D4	E2	7.0	0.35	0.63
10	A3	B2	C4	D3	E1	8.0	0.38	0.79
11	A3	B3	C1	D2	E4	9.5	0.41	1.0
12	A3	B4	C2	D1	E3	7.5	0.30	0.58
13	A4	B1	C2	D2	E3	6.0	0.28	0.39
14	A4	B2	C1	D1	E4	6.5	0.24	0.36
15	A4	B3	C4	D4	E1	7.5	0.35	0.68
16	A4	B4	C3	D3	E2	5.0	0.16	0.05
^a K ₁	0.348	0.293	0.543	0.410	0.468			
K ₂	0.455	0.575	0.365	0.533	0.430			
K ₃	0.750	0.730	0.405	0.383	0.580			
K ₄	0.370	0.325	0.610	0.598	0.445			
^b R	0.402	0.437	0.245	0.215	0.150			
Optimal level	A3	B3	C4	D4	E3			

^a $K_i^X = (\sum \text{the } H \text{ value of SDKP at } X_i)/4$.

^b $R_i^X = \max\{K_i^X\} - \min\{K_i^X\}$; *X* could be A, B, C, D, or E, and *i* could be 1, 2, 3, or 4.

Table VII. The Optimal Condition and the Performance of SDKP

Initiator concentration (%)	Reaction temperature (°C)	Mole ratio of NVCL/AMPS/DVB	SDS concentration (%)	pH	YP	YP/PV	H
0.20	65	60.0:38.0:2.0	2.0	7	10.5	0.43	1.14

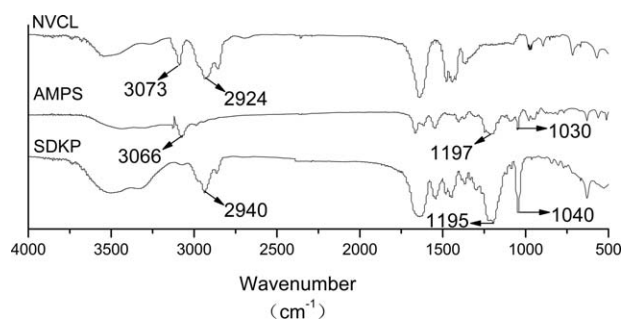
Performance Evaluation of SDKP in Drilling Fluid

To estimate the effectiveness of SDKP as viscosifier under different conditions, a series of drilling fluids with different SDKP concentrations were prepared. The HE300 was used as a comparison. The effects of aspects including the viscosifier amount, the aging temperature, and the salt content on the performance of fluids dealt with SDKP and HE300, was studied, respectively. Rheological properties (such as AV, PV, and YP) and filtrate properties (FL_{API} and FL_{HTHP}) of drilling fluids were measured before and after 230 °C hot rolling aging tests for 16h. The test results were illustrated in Tables (VIII and X) to X, respectively.

The impact of viscosifier concentration on the performance of drilling fluids was shown in Table VIII. Before and after thermal aging tests, all the rheological parameters of drilling fluids, including AV, PV, and YP, were greatly increased with the addition of SDKP or HE300 and further increased with the increments of viscosifier concentration. These results illustrated that the viscosifier contributed to the building up of the network structure, thus resulting in the viscosity-building ability. However, at the same dosage of 0.5%, 0.8%, or 1.0%, the rheological parameter values of the fluids dealt with SDKP before and after hot rolling aging tests were higher than the corresponding parameter values of the fluids dealt with HE300, which indicated that SDKP had better viscosity-building performance.

As shown in Table IX, HE300 had good viscosity-building ability when the temperature was not higher than 200 °C. However, its viscosity-building ability became significantly weak beyond that point. Compared with HE300, SDKP showed better thermal stability to elevated temperatures. For example, the rheological parameter values of the fluids dealt with SDKP remained high after hot rolling aging tests at 230 °C.

The effect of salinity on the performance of drilling fluids was shown in Table X. The fluids tended to thin when the salt was introduced, producing low AV, PV, and YP. These results illustrated that the salt impaired the network structure of fluids. However, at the same salinity of 8% or 36%, the rheological parameter values of the fluids dealt with SDKP before and after

**Figure 3.** FT-IR spectrum of AMPS, NVCL, and SDKP.

hot rolling aging tests were higher than the corresponding parameter values of the fluids dealt with HE300, which indicated the better salt tolerance of SDKP.

It could also be seen that the FL_{API} and FL_{HTHP} after the thermal aging test decreased with the addition of the viscosifier, and further decreased with the increase of SDKP or HE300 concentration, which indicated that the SDKP or HE300 also had a certain ability to reduce the fluid loss.

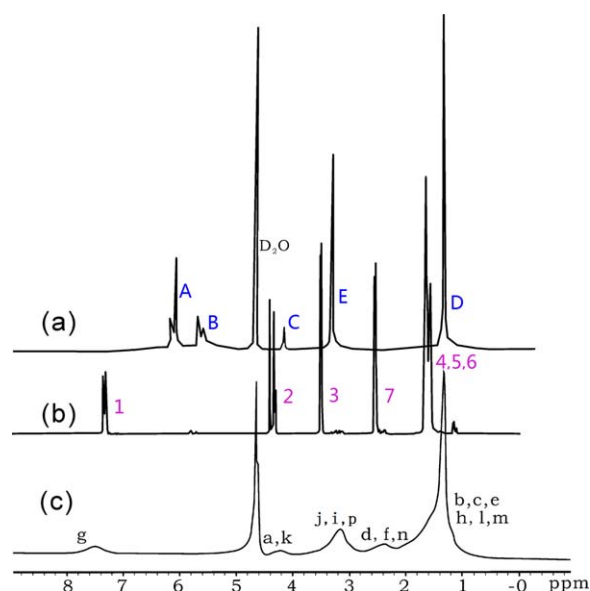
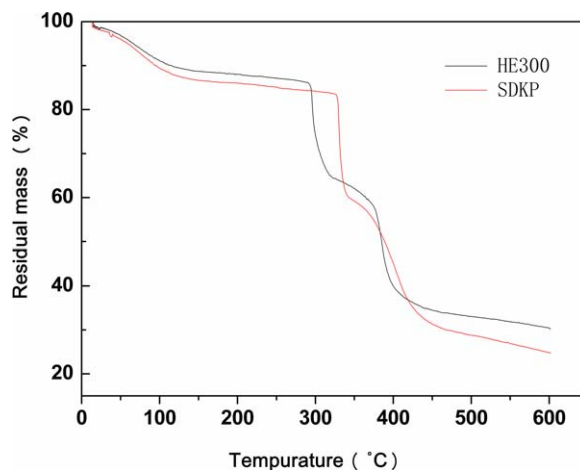
**Figure 4.** ¹H-NMR spectrum of AMPS, NVCL, and SDKP. [Color figure can be viewed in the online issue, which is available at wileyonlinelibrary.com.]**Figure 5.** Thermogravimetric curves of SDKP and HE300. [Color figure can be viewed in the online issue, which is available at wileyonlinelibrary.com.]

Table VIII. Effect of Viscosifier Dosages on Properties of Fluids

Fluid formulation	Hot rolling test	Typical rheological parameters						
		AV (mPa·s)	PV (mPa·s)	YP (mPa·s)	YP/PV	G_{10s}/G_{10min}	FL _{API}	FL _{HHTP}
LSFBF + 0.5% SDKP+ 0.5% Na ₂ SO ₃ + 6%SMP-II	Before	39.0	26.0	13.0	0.50	1.0/1.5	4.8	-
	After	30.0	21.0	9.0	0.43	0.5/0.75	8.6	25.8
LSFBF + 0.8% SDKP+ 0.5% Na ₂ SO ₃ + 6%SMP-II	Before	46.0	31.0	15.0	0.48	2.25/3.0	4.2	-
	After	34.5	23.5	10.5	0.45	1.5/2.0	8.2	22.0
LSFBF + 1.0% SDKP+ 0.5% Na ₂ SO ₃ + 6%SMP-II	Before	49.5	33.0	16.5	0.50	2.5/3.0	3.8	-
	After	36.5	24.0	12.5	0.52	2.0/2.5	6.6	19.6
LSFBF + 0.5% HE300+ 0.5% Na ₂ SO ₃ + 6%SMP-II	Before	35.0	24.0	11.0	0.46	1.0/1.5	6.2	-
	After	22.0	17.0	5.0	0.29	0.5/0.5	8.8	27.6
LSFBF + 0.8% HE300+ 0.5% Na ₂ SO ₃ + 6%SMP-II	Before	42.0	29.0	13.0	0.45	2.0/2.5	5.5	-
	After	24.5	18.0	6.5	0.36	0.5/1.0	9.0	21.5
LSFBF + 1.0% HE300+ 0.5% Na ₂ SO ₃ + 6%SMP-II	Before	46.5	32.0	14.5	0.45	2.0/2.5	4.6	-
	After	29.5	21.0	8.5	0.40	0.75/1.0	7.0	20.5

Rheological Properties under High Temperature and High Pressure

The HPHT rheological properties of viscosifier-containing fluids were shown in Figure 6. It was shown in Figure 6(a,b) that the Bingham plastic model was obviously suitable for the HPHT rheology profiles of viscosifier-containing fluids. The rheological parameter values (such as AV and YP) were determined based on Bingham plastic model. A comparison of rheological parameter values at different temperatures for the fluids was shown in Figure 6(c,d). The information summarized from Figure 6(c,d) was as follows. First, compared with HE300, the rheological parameter values of the fluids dealt with SDKP were much higher at the same temperature of 150 °C, 180 °C, or 220 °C, which showed that SDKP had better viscosity-building performance at HPHT conditions. Second, the response of the

rheological parameter values of viscosifier-containing fluids to increasing temperature was very different. In the case of HE300-containing fluids, the viscosity and yield stress displayed a continuous decrease with the temperature increased. However, the SDKP-containing fluids showed an increase in viscosity as the temperature increased except for 220 °C. This phenomenon could be explained as follows: *N*-vinylcaprolactam (NVCL) was family of the temperature sensitive monomer. The NVCL-based copolymers showed a Lower Critical Solution Temperature (LCST) in water.^{21,23,30} When the temperature was raised above the LCST of caprolactam (CL) units, these side chains could self-assemble into reversible hydrophobic association micro-domains which was accompanied by a change in the hydrodynamic volume of the polymer molecular in solution and the transition of a loose coil to a reticular aggregates.²³ Nevertheless, a macroscopic precipitation

Table IX. Effect of Aging Temperatures on Properties of fluids

Fluid formulation	Aging temperatures	Typical rheological parameters						
		AV (mPa·s)	PV (mPa·s)	YP (mPa·s)	YP/PV	G_{10s}/G_{10min}	FL _{API}	FL _{HHTP}
LSFBF + 0.8% SDKP+ 0.5% Na ₂ SO ₃ +6%SMP-II	Before	46.0	31.0	15.0	0.48	2.25/3.0	4.2	-
	180	44.0	30.0	14.0	0.47	2.0/2.5	5.4	18.8
	200	42.5	30.0	12.5	0.42	1.0/1.75	6.8	19.5
	230	34.5	23.5	10.5	0.45	1.0/1.5	8.2	22.0
LSFBF + 0.8% HE300+ 0.5% Na ₂ SO ₃ +6%SMP-II	Before	42.0	29.0	13.0	0.45	2.0/2.5	5.5	-
	180	34.0	22.5	11.5	0.51	1.0/1.5	6.0	17.8
	200	26.5	18.5	8.0	0.43	0.75/1.0	7.8	18.6
	230	24.5	18.0	6.5	0.36	0.5/1.0	9.0	21.5

Table X. Effect of Salinity on Properties of fluids

Fluid formulation	Hot rolling test	Typical rheological parameters						
		AV (mPa·s)	PV (mPa·s)	YP (mPa·s)	YP/PV	G_{10s}/G_{10min}	FL _{API}	FL _{HHP}
LSFBF + 0.8% SDKP + 0.5% Na ₂ SO ₃ + 6%SMP-II	Before	46.0	31.0	15.0	0.48	2.25/3.0	4.2	-
	After	34.5	23.5	10.5	0.45	1.5/2.0	8.2	22.0
LSFBF + 0.8% SDKP + 0.5% Na ₂ SO ₃ + 6%SMP-II + 8% NaCl	Before	39.5	28.0	11.5	0.41	1.75/2.0	4.8	-
	After	24.0	17.5	6.5	0.37	0.5/1.0	11.2	35.5
LSFBF + 1.3% SDKP + 0.5% Na ₂ SO ₃ + 6%SMP-II + 36% NaCl	Before	42.0	31.5	10.5	0.33	1.5/2.0	5.2	-
	After	20.0	16.0	4.0	0.25	0.5/0.5	14.6	43.8
LSFBF + 0.8% HE300 + 0.5% Na ₂ SO ₃ + 6%SMP-II	Before	42.0	29.0	13.0	0.45	2.0/2.5	5.5	-
	After	24.5	18.0	6.5	0.36	0.5/1.0	9.0	21.5
LSFBF + 0.8% HE300 + 0.5% Na ₂ SO ₃ + 6%SMP-II + 8% NaCl	Before	35.5	25.0	10.5	0.42	1.5/2.0	5.8	-
	After	20.5	15.0	5.5	0.37	0.5/0.5	10.8	41.8
LSFBF + 1.3% HE300 + 0.5% Na ₂ SO ₃ + 6% SMP-II + 36% NaCl	Before	37.5	25.0	12.5	0.50	1.5/2.0	5.4	-
	After	15.0	12.0	3.0	0.25	0.25/0.5	13.8	55.6

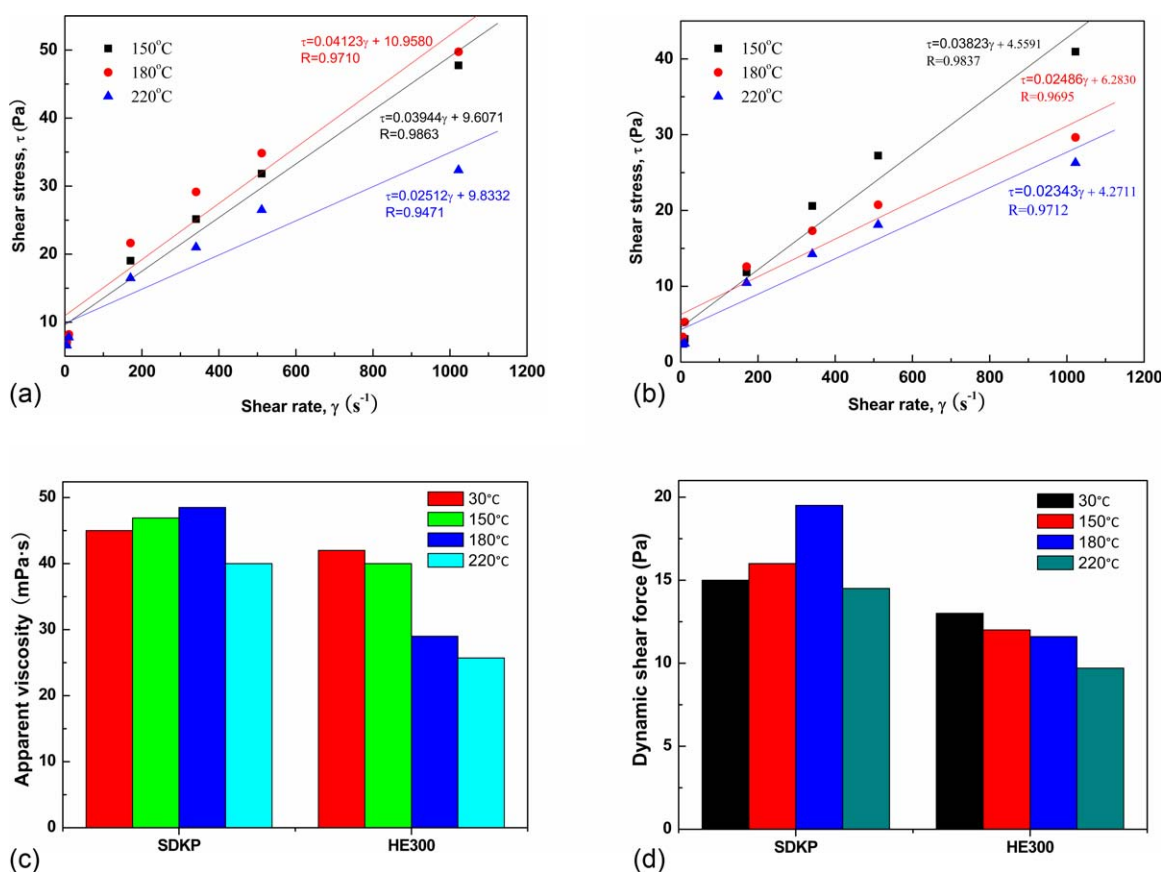


Figure 6. HPHT rheological properties of viscosifier-containing fluids. (a) Rheology profiles of SDKP; (b) Rheology profiles of HE300; (c) Effect of temperature on AV values; (d) Effect of temperature on YP values. Note: (1) Fluids composition was LSFBF + 0.8% viscosifier + 0.5%Na₂SO₃ + 6%SMP-II; (2) the value of AV and YP at 30°C was determined by ZNN-D6-type rotating viscometer, as described in Table VIII. [Color figure can be viewed in the online issue, which is available at wileyonlinelibrary.com.]

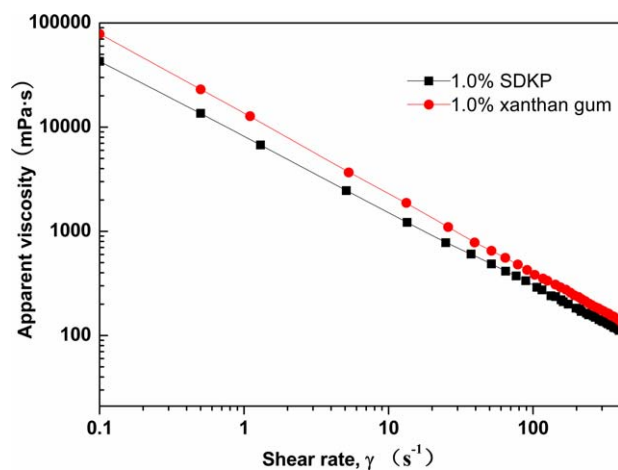


Figure 7. Shear-thinning properties of SDKP and xanthan gum aqueous solution. [Color figure can be viewed in the online issue, which is available at wileyonlinelibrary.com.]

or a phase separation was prevented by the hydrophilic backbones which stabilized the association phase at the microscopic level. The microdomains played the role of cross links between the polymeric chains, which would lead to the viscosity enhancement

significantly. However, in the much higher temperatures (220 °C), the hydrophobic aggregation structure was too strong which probably resulted in the precipitation of the polymer molecules.²³ So a decrease in viscosity at 220 °C was observed. The data from Figure 6 suggested that the viscosity and yield stress of SDKP-containing fluids at 220 °C was 31.5 mPa s and 14.5 Pa, respectively, which indicated that the SDKP-containing fluids had excellent high temperature associative thickening property.

Shear-Thinning Rheology of SDKP Aqueous Solution

The shear-thinning behavior of 1.0% (mass fraction) SDKP aqueous solution of at room temperature was illustrated in Figure 7. The 1.0% xanthan gum was used as a comparison.

As illustrated in Figure 7, the SDKP solution exhibited relatively low high-shear-rate viscosity (HSRV) in high-shear region and relatively high low-shear-rate viscosity (LSRV) in low-shear region. The data from Figure 7 suggested that the 1.0% SDKP solution could match the rheological properties of 0.5% xanthan gum solution. It was shown that the SDKP solution displayed clearly the shear-thinning rheological profiles as observed in xanthan gum solution, which was beneficial to reduce friction losses and hole cleaning.

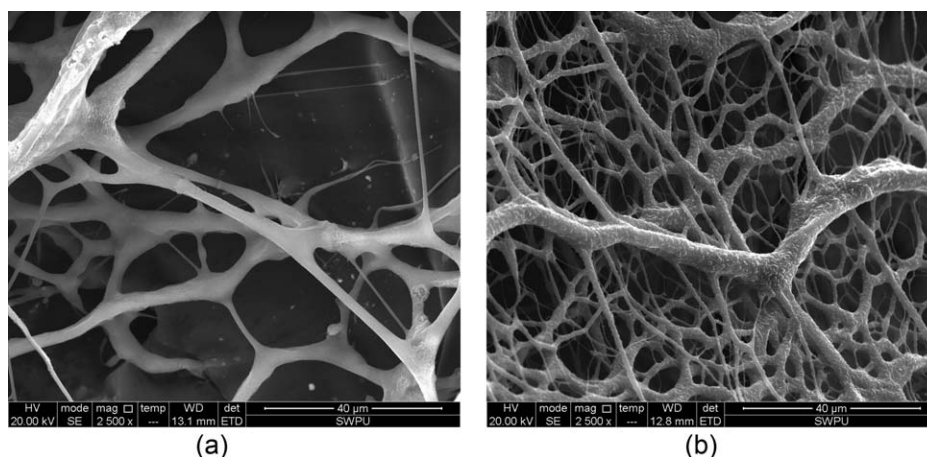


Figure 8. ESEM images of SDKP in aqueous solution (a) 0.25% SDKP; (b) 0.5% SDKP.

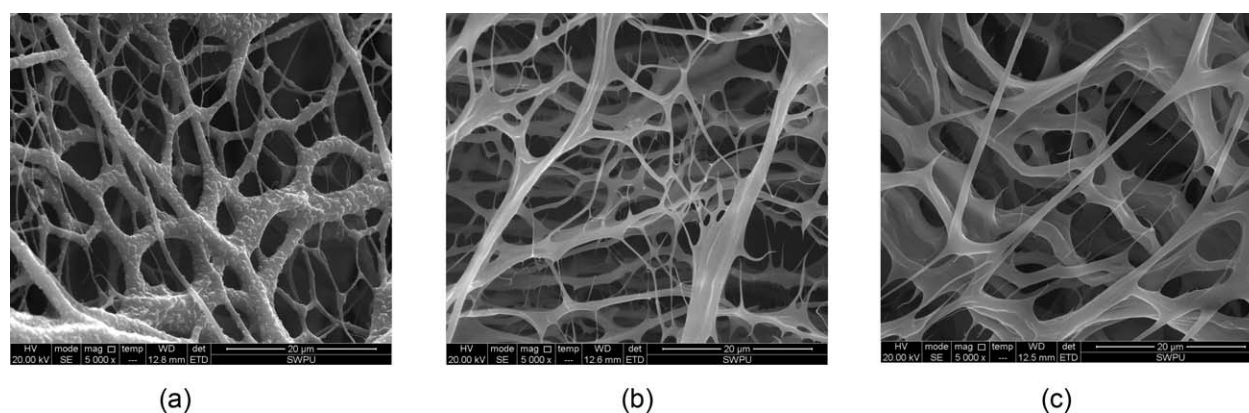


Figure 9. ESEM images of SDKP in NaCl solution (a) 0% NaCl; (b) 0.3% NaCl; (c) 1.0% NaCl.

The Microscopic Morphology of SDKP in Solution

To study the thickening mechanism of SDKP in aqueous solution and saline solution, environmental scanning electron microscope (ESEM) was used to observe the microscopic morphology of the SDKP solution.

Figure 8 displayed the aggregation conformation of SDKP in aqueous solution with different SDKP concentration. As shown in Figure 8, the continuous three-dimensional network was formed in SDKP aqueous solution because of the micro-crosslinked structure and intermolecular hydrophobic association of SDKP molecule, which leading to the good viscosity-building ability. With increasing SDKP concentration from 0.25% to 0.5%, the network skeleton became much larger and more compact and the diameter of network skeleton was about a few microns to more than ten microns in 0.5% SDKP aqueous solution, which resulting in the better thickening property.

The influence of salinity on the microscopic morphology of 0.5% SDKP solution was shown in Figure 9. As shown in Figure 9, with increasing salt concentration from 0 to 1.0%, a thick aggregate was gradually formed. This was because that both the hydrophobic group and the anionic group $-\text{SO}_3^-$ were present in the SDKP molecule. The anionic groups along the polymer chains were gradually shielded with increasing NaCl concentration, leading to the shrinkage of the polymer chains. At the same time, intermolecular associations of hydrophobic groups were reinforced due to the increase in polarity of brine solution, resulting in the enhanced association structures. Therefore, the SDKP had a relatively high viscosity in saline solution. As observed in Figure 9(c), the continuous networks spanned in 1% NaCl solution were still formed, indicating the good salt resistance behavior of SDKP.

CONCLUSIONS

A novel polymer viscosifier SDKP for aqueous bentonite drilling fluids was prepared with sodium 2-acrylamido-2-methylpropane sulfonate, *N*-vinylcaprolactam, and cross-linking divinylbenzene via micellar radical polymerization. The optimal SDKP was obtained under the optimum reaction conditions: initiator concentration (by weight of monomer) = 0.20%, reaction temperature = 65 °C, mole ratio of NVCL/AMPS/DVB = 60.0:38.0:2.0, SDS concentration (by weight of monomer) = 2.0%, and pH value = 7. The structure of SDKP was characterized by FT-IR, $^1\text{H-NMR}$, elemental analysis, and GPC. The evaluation results for SDKP containing drilling fluid have demonstrated that SDKP had excellent thickening property, resistance to elevated temperature, salt tolerance, and shear thinning property. Unlike common viscosifier, the SDKP displayed a thermo-thickening effect in temperature range of 150 to 180 °C, which was beneficial to increase the viscosity and strength of fluids at high temperatures. This showed a potential use when applied to HTHP wells. Furthermore, the thickening mechanism of SDKP at room temperature was discussed by means of ESEM observations.

ACKNOWLEDGMENTS

We would like to thank the financial support from the National Natural Science Foundation of China (No. 51404040) for this work.

REFERENCES

1. James, R. W.; Schei, T.; Navestad, P.; Geddes, T. M. *SPE Drill. Compl.* **2000**, *15*, 254.
2. Amanullah, M.; Yu, L. *J. Pet. Sci. Eng.* **2005**, *48*, 199.
3. Stamatakis, E.; Young, S.; Stefano, G. D. Presented at the SPE Oil and Gas Conference and Exhibition in Mumbai, India, **2012**; SPE paper 153709.
4. Thaemlitz, C. J.; Coffin, G.; Conn, L. *SPE Drill. Compl.* **1999**, *14*, 185.
5. Tehrani, A.; Gerrard, D.; Young, S.; Fernandez, J. Presented at the SPE International Symposium on Oilfield Chemistry in Woodlands, Texas, USA, **2009**; SPE paper 121783.
6. Tehrani, M. A.; Popplestone, A.; Guarneri, A.; Carminati, S. Presented at the SPE International Symposium on Oilfield Chemistry in Houston, Texas, USA, **2007**; SPE paper 105485.
7. Zheng, J.; Wang, J. Z. Presented at the SPE Middle East Oil and Gas Show and Conference in Manama, Bahrain, **2011**; SPE paper 142099.
8. Berry, J. E.; Thomas, E. W. Presented at the IAOC/SPE Drilling Conference in Dallas, Texas, USA, **1994**; SPE paper 27453.
9. Mahto, V.; Sharma, V. P. *J. Petrol. Sci. Eng.* **2004**, *45*, 123.
10. Hamed, S. B.; Belhadri, M. *J. Petrol. Sci. Eng.* **2009**, *67*, 84.
11. Sabhapondit, A.; Borthakur, A.; Haque, I. *J. Appl. Polym. Sci.* **2003**, *87*, 1869.
12. Sabhapondit, A.; Borthakur, A.; Haque, I. *Energy Fuels* **2003**, *17*, 683.
13. Audibert, A.; Argillier, J. F. Presented at the SPE International Symposium on Oilfield Chemistry in San Antonio, TX, USA, **1995**; SPE paper 28953.
14. Podhajecka, K.; Prochazka, K.; Hourdet, D. *Polymer* **2007**, *48*, 1586.
15. Volpert, E.; Selb, J.; Candau, F. *Polymer* **1998**, *39*, 1025.
16. Cao, J.; Tan, Y. B.; Che, Y. J.; Ma, Q. *J. Polym. Res.* **2011**, *18*, 171.
17. Gouveia, L. M.; Grassl, B.; Alejandro, J.; Müller, J. *Colloid Interface Sci.* **2009**, *333*, 152.
18. Rashidi, M.; Blokhuis, A. M.; Skauge, A. J. *J. Appl. Polym. Sci.* **2011**, *119*, 3623.
19. Yan, L. L.; Wang, C. B.; Xu, B.; Sun, J. S.; Yue, W.; Yang, Z. *X. Mater. Lett.* **2013**, *105*, 232.
20. Bai, X. D.; Yang, Y.; Xiao, D. Y.; Pu, X. L.; Wang, X. *J. Appl. Polym. Sci.* **2015**, *132*, DOI: 10.1002/app.41762.
21. Thaemlitz, C. J. U.S. Pat. 7,098,171 (**2006**).
22. Makhaeva, E. E.; Tenhu, H.; Khokhlov, A. R. *Macromolecules* **2002**, *35*, 1870.

23. Xie, B. Q.; Qiu, Z. S. *Polym. Mater. Sci. Eng.* (in Chinese) **2014**, *30*, 73.
24. Zhong, C. R.; Ye, L.; Dai, H.; Huang, R. H. *J. Appl. Polym. Sci.* **2007**, *103*, 277.
25. Okhapkin, I. M.; Nasimova, I. R.; Makhaeva, E. E.; Khokhlov, A. R. *Macromolecules* **2003**, *36*, 8130.
26. Yanul, N. A.; Kirsh, Y. E.; Verbrugghe, S.; Goethals, E. J. D.; Prez, F. E. *Macromol. Chem. Phys.* **2001**, *202*, 1700.
27. Laukkanen, A.; Winnik, F. M.; Tenhu, H. *Macromolecules* **2005**, *38*, 2439.
28. Guo, S. L.; Bu, Y. H. *J. Appl. Polym. Sci.* **2013**, *127*, 3302.
29. Mao, H.; Qiu, Z. S.; Shen, Z. H. *J. Petrol. Sci. Eng.* **2015**, *129*, 1.
30. Makhaeva, E. E.; Tenhu, H.; Khokhlov, A. R. *Macromolecules* **1998**, *31*, 6112.